ISTITUTO NAZIONALE DI FISICA NUCLEARE

Sezione di Torino

INFN/AE-90/03
27 Aprile 1990

C. Biino, S. Palestrini:

SENSITIVITY TO MIXING AND CP VIOLATIONS IN THE B°-$\bar{B}^{\circ}$ SYSTEM BY DECAY DISTRIBUTION STUDY

Servizio Documentazione
dei Laboratori Nazionali di Frascati

INFN - Istituto Nazionale di Fisica Nucleare
Sezione di Torino

INFN/AE-90/03
27 Aprile 1990

SENSITIVITY TO MIXING AND CP VIOLATION IN THE B^0-$\overline{B}^0$ SYSTEMS BY DECAY DISTRIBUTION STUDY

Cristina Biino and Sandro Palestini
INFN - Sez. di Torino, Via P.Giuria 1, 10125 Torino (Italy)

ABSTRACT

The subjects of B_s-$\overline{B}_s$ mixing and time dependent CP violation in B^0 ($\overline{B}^0$) decays are discussed, evaluating the requirements necessary for measurements based on decay distribution analysis. Inclusive B-$\overline{B}$ production is assumed.

1. - INTRODUCTION

The study of the decay of mesons containing the quark "beauty" provides relevant tests to the standard model of the weak interactions. In recent years, the measurement of several B-mesons branching ratios[1] allowed to determine or to place constraints[2] on several elements of the Cabibbo-Kobayashi-Maskawa (CKM) matrix;[3] the study of the decay of B-$\overline{B}$ pairs has shown the existence of significant mixing between the $B_d(d\overline{b})$ and $\overline{B}_d(\overline{bd})$ states.[4] This effect, which is expected to be present in the B_s-$\overline{B}_s$ system too, may provide

a mechanism for measurable violations of CP symmetry, which so far have been detected in the K^o-$\overline{K}^o$ system only.

The subjects of B^o-$\overline{B}^o$ mixing,[5-6] the detection of B_s-$\overline{B}_s$ oscillations,[7-8] and the violation of CP symmetry in B^o ($\overline{B}^o$) decays,[9-11] have been studied by several authors. So far, the main interest has been on time integrated analyses, i.e. on the measurement of branching ratios. Furthermore, most analyses refers to B-$\overline{B}$ pairs produced in the decay of "bottomonium" (Y-family) particles. In fact, most of the experimental results collected so far were obtained with techniques satisfying at least one of these conditions.

In this paper, we analyze the possibility of detecting B_s-$\overline{B}_s$ mixing and decay time dependent CP violation in the B^o-$\overline{B}^o$ systems. We assume that the beauty mesons are produced incoherently, and that measurements of decay times are performed. These conditions can be satisfied, for example, in studies of hadronic production of Beauty in dedicated detectors, or for B-mesons from the decay of Z^o's at electron-positron colliders.

In the following sections, we discuss separately the issues of flavor mixing and CP violation. In each case, we briefly review the formalism and expectations of the Standard Model, discuss typical experimental conditions, and show results based on analytical and Monte Carlo calculations.

2. - REVIEW OF FLAVOR OSCILLATION FORMALISM

The decay of neutral B-mesons $B_q(q\overline{b})$ and $\overline{B}_q(b\overline{q})$, q=d or s, is determined by a 2x2 hamiltonian matrix:

$$H = M - \frac{i}{2}\Gamma \ , \tag{2.1}$$

where M and Γ are hermitian matrices; we use the basis vectors:

$$|B^o\rangle = \begin{bmatrix}1\\0\end{bmatrix} \ , \quad |\overline{B}^o\rangle = \begin{bmatrix}0\\1\end{bmatrix} \quad ; \tag{2.2}$$

CPT invariance implies that:

$$H_{11} = H_{22} \equiv m - \frac{i}{2}\gamma \ . \tag{2.3}$$

The eigenstates of (2.1) can be parametrized as :

$$|B_H\rangle \equiv p\,|B^o\rangle - q\,|\overline{B}^o\rangle \quad , \quad |B_L\rangle \equiv p\,|B^o\rangle + q|\overline{B}^o\rangle \tag{2.4}$$

where H and L stand for heavy and light; the corresponding eigenvectors are:

$$\mu_{H,L} \equiv m_{H,L} - \frac{i}{2}\gamma_{H,L} = m - \frac{i}{2}\gamma \pm \frac{1}{2}\Delta\mu \ , \tag{2.5}$$

with:

$$\Delta\mu \equiv \pm (-2)\sqrt{\left(M_{12}^* - \frac{i}{2}\Gamma_{12}^*\right)\left(M_{12} - \frac{i}{2}\Gamma_{12}\right)} \ ; \tag{2.6}$$

the coefficients p, q satisfy:

$$\frac{q}{p} = \frac{-\Delta\mu}{2\,(M_{12} - \frac{i}{2}\Gamma_{12})} = \pm\left(\frac{M_{12}^* - \frac{i}{2}\Gamma_{12}^*}{M_{12} - \frac{i}{2}\Gamma_{12}}\right)^{1/2} . \tag{2.7}$$

At production time (t=0) the beauty neutral mesons are pure B^o, $\overline{B}^o$ states. The time evolved $B^o_{phys}(t)$ [$\overline{B}^o_{phys}(t)$] corresponding to $B^o(0)$ [$\overline{B}^o(0)$] are superpositions of B_H , B_L states. In terms of the time independent B^o, $\overline{B}^o$ beauty eigenstates, the time evolution is described by:

$$|B^o_{phys}(t)\rangle = e^{-imt-\gamma t/2}\left[\cos\frac{\Delta\mu\cdot t}{2}\,|B^o\rangle + \frac{q}{p}\,i\sin\frac{\Delta\mu\cdot t}{2}\,|\overline{B}^o\rangle\right] \tag{2.8}$$

$$|\overline{B}^o_{phys}(t)\rangle = e^{-imt-\gamma t/2}\left[\frac{p}{q}\,i\sin\frac{\Delta\mu\cdot t}{2}\,|B^o\rangle + \cos\frac{\Delta\mu\cdot t}{2}\,|\overline{B}^o\rangle\right] \tag{2.9}$$

In the standard model, the off-diagonal elements of H are determined by the "box diagrams",(6) shown in Figure 1. At each vertex, a $W^{\pm}$ is attached with coupling proportional to the corresponding coefficients V_{ij} of the CKM matrix; therefore the amplitude of the diagrams is proportional to $V_{q'q}V_{q'b}^*V_{q''q}V_{q''b}^*$, summing over the flavor indices q', q". Notice that in the limit of equal quark masses, the unitarity of V_{ij} makes the sum vanish. For different masses, the largest kinematic contribution is provided by the heaviest quark, i.e. the predicted "top" quark, so that:

$$\Delta\mu \propto m_t^{\,2}\,(V_{tq}\,V_{tb}^*)^2 \ . \tag{2.10}$$

Notice that since a B-meson cannot decay in a system containing a t-quark, the expression (2.10) contributes only to the non-absorptive part of the mass matrix, so that:

$$|M_{12}| \gg |\Gamma_{12}| \quad . \tag{2.11}$$

(In fact it can be shown that $|\Gamma_{12}/M_{12}| \approx (m_b/m_t)^2$ [6]). Relation (2.11) allows to approximate (2.6-7) with the expressions:

$$\Delta\mu \equiv \Delta m \equiv 2\,|M_{12}| \quad , \quad \Delta\gamma \equiv 0 \quad , \quad \left|\frac{q}{p}\right| \equiv 1 \quad . \tag{2.12}$$

Under these approximations, B_H and B_L have identical lifetimes, and (2.8-9) can now be rewritten as:

$$|B^o_{phys}(t)> \equiv e^{-imt-\gamma t/2}\left[\cos\frac{\Delta m\cdot t}{2}\,|B^o> + i\,\sin\frac{\Delta m\cdot t}{2}\,|\overline{B}^o>\right] \quad , \tag{2.8'}$$

$$|\overline{B}^o_{phys}(t)> \equiv e^{-imt-\gamma t/2}\left[i\,\sin\frac{\Delta m\cdot t}{2}\,|B^o> + \cos\frac{\Delta m\cdot t}{2}\,|\overline{B}^o>\right] \quad , \tag{2.9'}$$

where we have made the conventional choice:[12]

$$\frac{p}{q} \equiv 1 \quad . \tag{2.13}$$

The squares of the amplitudes (2.8'), (2.9') are the time-dependent probabilities for flavor non-oscillation and oscillation:

$$\frac{d\Gamma(B^o_{phys}\to B^o)}{dt} \equiv \frac{d\Gamma(\overline{B}^o_{phys}\to \overline{B}^o)}{dt} \equiv e^{-\gamma t}\frac{1}{2}\,[\,1 + \cos(\Delta m\cdot t)\,], \tag{2.14}$$

$$\frac{d\Gamma(B^o_{phys}\to \overline{B}^o)}{dt} \equiv \frac{d\Gamma(\overline{B}^o_{phys}\to B^o)}{dt} \equiv e^{-\gamma t}\frac{1}{2}\,[\,1 - \cos(\Delta m\cdot t)\,] \quad . \tag{2.15}$$

We use the "oscillation parameter" $x_q \equiv \Delta m/\gamma$ (which is proportional to the lifetime to oscillation period ratio), where q refers to the light quark flavor d or s, and we measure time in lifetime units (γ=1). Hence (2.14-15) can be written in the form:

$$\frac{d\Gamma(t,\pm)}{dt} \equiv e^{-t}\frac{1}{2}\,[\,1 \pm \cos(x_q\cdot t)] \quad , \tag{2.16}$$

where the sign (+) applies to beauty conservation ($B^o_{phys}(t)\to B^o$ and $\overline{B}^o_{phys}(t)\to \overline{B}^o$), the sign (-) to B-$\overline{B}$ oscillation ($B^o_{phys}(t)\to \overline{B}^o$ and $\overline{B}^o_{phys}(t)\to B^o$).

From (2.10) one can predict:

$$\frac{x_s}{x_d} \cong \left|\frac{V_{ts}}{V_{td}}\right|^2 \quad . \tag{2.17}$$

From our knowledge of the CKM coefficients,[2] the measurement of B_d-$\overline{B}_d$ oscillations,[4] and theoretical corrections and uncertainties in (2.17), it has been estimated that $x_s > 3$ (90% C.L.).[13] Fig. 2 shows the non-oscillating and the oscillating decay time distributions for x=0.7 (B_d) and x=10 .

3. - MEASUREMENT OF B-$\overline{B}$ OSCILLATIONS

In order to study beauty oscillations, one has to compare the beauty quantum numbers of a neutral B-meson at formation and at decay. The latter observation requires the reconstruction of the decay mode, while the former is obtained in a similar way by looking at the decay of the associated hadron containing a b-quark ($\overline{b}$). Obviously we are considering b-$\overline{b}$ production in a flavor conserving strong or electromagnetic process.

Let us consider first the case of a neutral B-meson produced together with a $B^{\pm}$-meson. Beauty oscillation manifests in the presence of final states with beauty number equal to ± 2, such as B^+-B^o or B^--$\overline{B}^o$. The oscillation is usually described by the parameter r : [14]

$$r \equiv \frac{\Gamma(B^o \to \overline{B}^o)}{\Gamma(B^o \to B^o)} \cong \frac{\Gamma(\overline{B}^o \to B^o)}{\Gamma(\overline{B}^o \to \overline{B}^o)} \quad , \tag{3.1}$$

where the second equality holds in the approximation $|p/q| \cong 1$. Integrating the decay distributions (2.16), it can be shown that :

$$r = \frac{x_q^2}{2+x_q^2} \quad . \tag{3.2}$$

Alternatively, the variable χ is used:

$$\chi \equiv \frac{\Gamma(B^o \to \overline{B}^o)}{\Gamma_{tot}(B^o)} \cong \frac{\Gamma(\overline{B}^o \to B^o)}{\Gamma_{tot}(\overline{B}^o)} \quad , \tag{3.3}$$

which is related to r by: $\chi = r / (1+r)$.

Time integrated analyses provide the value of:

$$R \equiv \frac{N(B^o\text{-}B) + N(\overline{B}^o\text{-}\overline{B})}{N(B^o\text{-}\overline{B}) + N(\overline{B}^o\text{-}B)} \qquad (3.4)$$

where, for example, $N(B^o\text{-}B)$ is the number of events containing a B^o together with another particle containing a $\overline{b}$ quark: $B^+=B_u$, B_d , B_s or $\overline{\Lambda}_b$. The parameter R is related to r,[15] and therefore to x. In the B_d case, the measurements of ARGUS and CLEO [4] allow to establish $x_d=0.70\pm0.13$.

In the case of B_s, however, the oscillation parameter x_s is presumably much larger than unity, and the time-integrated parameter is close to the saturation value: $r \equiv 1$ ($\chi \equiv 0.5$). In this situation, the observation of 1000 B_s , background free, could only allow to place a lower bound $x_s > 4.3$ (90% C.L., for $x_s \approx 10$ or larger).

Therefore time-integrated analyses are not effective for the measurement of x_s; we shall show below that time-dependent techniques, based on the same statistical sample of the example above, can reach resolution on x_s of the order of 0.1 . This approach requires the measurement of the B_s pathlength in accurate vertex detectors. Notice that this is not possible at electron-positron colliders running at the Y-family resonances, since B-mesons are produced almost at rest.[16]

We now discuss some aspects of oscillation analysis, focussing on time-dependent techniques, although some observations may also be applied to the time-integrated approach.

Tagging the B_s / $\overline{B}_s$ character at production by fully reconstructing associated $B^{\pm}$ states is not convenient, since the efficiency for beauty particle reconstruction is low, as discussed below in Section 6, and very small statistical samples would be available in this way.

We shall consider the case where the B_s-meson ($\overline{B}_s$) is fully reconstructed (this allows to discriminate among B_s, B_u and B_d, and to obtain the decay time from the pathlength and the total momentum of the decay products), while the associated (anti)beauty-particle is only partially reconstructed, and tagging is assigned looking at characteristics of the decay products correlated to the beauty quantum number. We refer to this approach as "inclusive tagging".

Various tagging techniques are possible. For instance, one can consider semileptonic decays, corresponding to the quark subprocess $b \rightarrow q\, l^- \overline{\nu}$, where q = c or u, and use the lepton sign to determine the beauty number [4,17-18]. The identification of charm in the final state is another possible technique, since the dominant decay is $b \rightarrow c\, X$. One step further, it is conceivable to look at strangeness in the final state,[19] given the dominant charm decay: $c \rightarrow s\, X$. If the associated beauty hadron (the "tagging" particle) is a beauty baryon, one can also rely on the identification of the nucleon in the final state.

Our sample of inclusively tagged B_s ($\overline{B}_s$) will include events with two neutral beauty mesons, i.e. pairs produced as B_s-$\overline{B}_s$, B_s-$\overline{B}_d$ and charge conjugated states, where both members are subjected to particle-antiparticle oscillations. The decay distribution expression (2.16) must be modified according to:

$$\frac{d\Gamma(t,\pm)}{dt} = e^{-t}\frac{1}{2}[\,1 \pm \alpha_1 \cos(x_q \cdot t)] \quad , \tag{3.5}$$

where $\alpha_1 < 1$ is given by:

$$\alpha_1 \equiv \Sigma_i\, f_i(1-2\chi_i) = \Sigma_i \frac{f_i}{1+x_i^2} \quad , \tag{3.6}$$

where the index i runs over the possible tagging particles: B_u, B_d, B_s and Λ_b, characterized by the corresponding oscillation parameters $\chi_i = 0, \cong 0.2, 0.5$ (expected), 0 respectively, and by the appropriate fragmentation fractions f_i describing the probability for a quark b to hadronize into the different ("stable") beauty particles. The expectation [20] is $f_u \cong f_d \cong 0.37$, $f_s \cong 0.18$, $f_\Lambda \cong 0.08$, resulting in $\alpha_1 \cong 0.67$.

4. - DETECTOR QUALITY FACTORS

The amplitude of the oscillating term in (3.5) is significantly affected by experimental conditions. For instance, different detector acceptance, or reconstruction efficiency, for the various tagging particles will affect (3.6). Furthermore, tagging inaccuracy and limited decay time resolution effectively reduce the oscillation amplitude, as discussed in some details in this section.

Consider the lepton tagging. This is the technique most frequently used so far. Its validity is based on two detector characteristics: a) quality of lepton identification, b) ability in discriminating events in which the electron is produced in a beauty semileptonic decay from

those in which the lepton comes from the decay of a charmed state originated in the beauty decay, which typically result in erroneous tagging. In experiments where beauty pairs are produced inclusively, a further requirement is the capability of rejecting leptons not associated with beauty decay. Similar consideration can be applied to the other inclusive tagging techniques discussed above.

Erroneous tagging reduces the effective value of the oscillation amplitude. If f_{mt} is the "mistagging" probability, then (3.5) is replaced by:

$$\frac{d\Gamma(t,\pm)}{dt} = e^{-t}\,\frac{1}{2}\{[\,1 \pm \alpha_1 \cos(x_q\cdot t)]\cdot(1-f_{mt}) + [\,1 \mp \alpha_1 \cos(x_q\cdot t)]\cdot f_{mt}\}$$

$$= e^{-t}\,\frac{1}{2}[\,1 \pm \alpha_1\cdot\alpha_2 \cos(x_q\cdot t)] \quad , \qquad (4.1)$$

with α_2 defined by:

$$\alpha_2 \equiv (1-2\cdot f_{mt}) \quad . \qquad (4.2)$$

A further reduction in the oscillation amplitude is due to limited resolution in decay time. Assuming that the error in measuring t is distributed as a gaussian with rms width σ_t, the effective distribution of the reconstructed events will be:

$$N(\,t\,,\pm\,,\alpha,\sigma_t)=N_0\int_0^{\infty}\exp\left[\frac{-(t'-t)^2}{2\sigma_t^2}\right]e^{-t'}\,\frac{1}{2}[1 \pm \alpha\,\cos(x\cdot t')]\,\varepsilon(t')\,dt' \quad , \qquad (4.3)$$

where $\alpha = \alpha_1\cdot\alpha_2$, $\varepsilon(t)$ is the effective detector acceptance, which depends on the decay time, and N_0 is the total number of produced events. We assume that the acceptance ε is approximately equal to the constant ε_C for decay time larger than a few times σ_t; then for t larger than a few σ_t's, the integral in (4.4) can be computed directly, obtaining the expression:

$$N(\,t\,,\pm\,,\alpha\,,\sigma_t) \equiv N_0\exp(-t+\sigma_t^2/2)\,\frac{1}{2}[1 \pm \alpha\cdot e^{-\sigma_t^2 x^2/2}\cdot\cos(x\cdot t - \sigma^2 x)]\,\varepsilon_C \quad . \qquad (4.4)$$

The most relevant result is that limited resolution in the decay time adds a further reduction factor to the oscillating term:

$$\alpha_3 \equiv \exp\left[-(\sigma_t\cdot x)^2/2\right] \quad . \qquad (4.5)$$

Notice that α_3 depends on the oscillation parameter x. Present vertex detectors technology should allow values $\sigma_t \approx 0.1 \cdot \tau \cong 0.12$ psec. For such small errors in t, the approximations used above should be valid for a large fraction of the collected events, and the vertex resolution becomes a limiting factor only for $x > 10$.

The apparent decay distributions will be also affected by background. We have assumed that a full reconstruction of the B_s meson is achieved, so that the background due to B_d or B_u is kept at low level.[21] Full simulation of a realistic detector showed that this condition can be achieved optimizing vertex reconstruction, momentum measurement and particle identification, even in the high multiplicity environment of hadronic colliders.[19,22]

5. - SIMULATED ANALYSIS RESULTS

In order to evaluate the sample (N) of tagged B_s needed to measure the oscillation parameter x_s, we simulated decay time distribution analyses for different values of oscillation parameter, sample size, and detector characteristics. The simulation accounted for mistagging and limited decay time resolution. The maximum likelihood technique was used to fit for decay time distribution of the form:

$$e^{-t} \frac{1}{2} [1 \pm \alpha \cos(x_s \cdot t)] \qquad (5.1)$$

where the parameter a includes the effects of: a) oscillating tagging particle, b) mistagging, c) limited decay time distribution. In the notation of the preceding section:

$$\alpha \equiv \alpha_1 \cdot \alpha_2 \cdot \alpha_3 \quad . \qquad (5.2)$$

For short decay times, the efficiency is expected to be small because of cuts necessary to separate the decay vertex from the primary interaction vertex. We accounted for this effect introducing a smooth efficiency function $\varepsilon(t)$ varying from $\varepsilon=0$ for $t < 0.2$, to $\varepsilon=1$ for $t > 1.0$, in lifetimes units. We also took into account the phase delay introduced by the limited decay time resolution (4.4), but it had negligible effects, for our σ_t values.

The minimization algorithm [23] optimized the values of x_s and α; we did not let the lifetime be fitted at the same time, since its value should be determined with high accuracy using the larger sample of B_s events not subjected to the tagging requirement. A similar consideration applies to the experimental uncertainty in $\varepsilon(t)$.

In order to test the reliability of the technique, we looked for spurious solutions corresponding to values of x_S and α away from the generated value. For the event samples and choice of parameters used in the analysis, all these secondary maxima had likelihood lower than the solution in the proximity of the generated values (L_O), and their significance can be characterized by the value of the parameter:

$$\Delta_S \equiv \sqrt{2(L_O - L_S)} \quad , \tag{5.3}$$

where L_S is the largest likelihood value among the spurious solutions. Δ_S can be interpreted as the number of standard deviations separating the correct solution from the most likely spurious one.

Table I shows results for Δ_S and for the rms uncertainty σ_x in the fitted value of x, obtained under different assumptions. In each case, 10 independent tries were performed. We found that all the fits were substantially unbiased, and that the errors σ_x and σ_α were good estimates of the residuals between generated and fitted values. The two errors were found to be correlated to a level of a few percent only. The value of σ_α is typically large when compared with the expectation range for α_1 and reasonable experimental uncertainties in the determination of α_2 and α_3 , therefore this technique is accurate in determining the oscillation parameter x, but rather weak in the measurement of the effective oscillation amplitude.

We found that our results are well approximated (<10% inaccuracy) by the semi-empirical formulae:

$$\sigma_x \cong \frac{0.8}{\alpha\sqrt{N}} \quad , \tag{5.4}$$

$$\Delta_S \cong 0.6\,\alpha\sqrt{N} \quad , \tag{5.5}$$

despite the wide range of parameter used (α from 0.16 to 0.8, N from 40 to 2800). Notice that if we require $\Delta_S > 4$, in order to discard spurious solutions to a C.L. corresponding to 4 σ, then we find $\sigma_x < 0.12$; assuming (conservatively) the value $\alpha \approx 0.2$, the corresponding required statistical sample size is $N_{min} \approx 1100$.

6. - CONCLUSIONS ON B_S-$\overline{B}_S$ OSCILLATIONS

In the preceding section we have shown that samples of the order of 1000 reconstructed and tagged B_S ($\overline{B}_S$) mesons are necessary in order to reach the statistical sensitivity required for an accurate measurement of x_S. We assumed that the B_S sample is essentially background free, and discussed the effect of looser requirements on the reconstruction of the tagging beauty partner. As shown in (5.4-5), the necessary statistical sample size is strongly correlated with tagging quality (3.6, 4.2), and, for large values of x_S, with the decay time resolution (4.5). In order to establish if this measurement is within the reach of present or near future experimental programs, we should discuss experimental techniques to a level of detail beyond the purpose of this report. We shall limit to a few observations and order of magnitude estimates.

Until now,[1,24] the only fully reconstructed B-mesons decays were obtained for B_u and B_d and corresponding charge conjugated states. The largest contributions to the total widths come from decays of the form: $\overline{B} \rightarrow D^* + n\ \pi$'s , $D + n\ \pi$'s , with $D = D^o, D^+$, and $n \leq 3$. We assume that the situation is similar for the B_S case, with D, D* replaced by D_S, D_S*, for a total reconstructible width approximately equal to 10%. All the D_S* are expected to decay into $D_S\ \gamma$, while the fraction of identified D_S decays is 22%.[24] Combining the B_S and D_S branching ratios, we assume that $\approx 2\%$ of the B_S decays are potentially reconstructible, in the sense that they involve final state configurations which have been handled with existent techniques.

We consider detectors with essentially full geometrical acceptance. Tagging efficiency is assumed to be equal to ≈10%. Further losses are due to vertex separation and quality cuts, where we assume a total factor 1/4. Finally, we must consider a final factor 1/3 for the probability of finding a B_S or $\overline{B}_S$ in the fragmentation products of a $b\text{-}\overline{b}$ quark pair.[25]

Under these assumptions, the sample of $b\text{-}\overline{b}$ recorded events necessary in order to extract 1000 tagged B_S's (or $\overline{B}_S$'s) is equal to $\approx 5 \cdot 10^6$. Trigger losses can be neglected for experiments running at Z^o factories, while the trigger efficiency is probably in the range 1-10 % in the other cases. These figures suggest that the measurement of x_S should be possible at dedicated detector at current high energy hadronic colliders,[19,22,26] while the luminosity might result too low at Z^o factories.[8] A general estimate is most uncertain for fixed target hadronic experiments, where the cross section ratio $\sigma(b\text{-}\overline{b})/\sigma_{tot}$ is very small, and our efficiency values may result optimistic.

7. - CP VIOLATION IN THE B^o SYSTEMS

CP violating effects may take place in the B mesons system through several mechanisms. First of all, CP violation is expected to be present in the mass matrix, manifesting as $|p/q| \neq 1$, in the notations of Section 2. These are usually called "indirect" CP violating effects, similar to those in the K^o system. However, the Standard Models predicts a very small effect of this kind,[27] for the measured values of the coefficients of the CKM matrix and the limits on the top quark mass.

A second class of CP violating effects is expected when a decay $B \rightarrow f$ (and its charge conjugated $\overline{B} \rightarrow \overline{f}$) takes place through two different amplitudes, with different combinations of CKM coefficients.[10] Notice that this "direct" CP violation effects may be experienced by charged states (B_u) also.

A sub-class of these effects consists of processes in which one of the two diagrams involves a B-$\overline{B}$ oscillation.[11] These are time-dependent CP violation effects, since different decay time distributions for the processes $B^o \rightarrow f$ and $\overline{B}^o \rightarrow \overline{f}$ are determined. As we shall discuss in more detail below, in the case of B_s the oscillation is expected to be fast enough to suppress time-integrated asymmetries.

In the following sections, we consider this last kind of CP violation effects only, and evaluate the possibility of detection in the near future. Since various fundamental and technical aspects are common to the topic of B-$\overline{B}$ oscillations, such as tagging and decay time resolution, we use notations and results from the previous sections.

8. - REVIEW OF FORMALISM

The decay time distributions of the processes $B^o_{phys} \rightarrow f$ and $\overline{B}^o_{phys} \rightarrow \overline{f}$, where B^o_{phys} [$\overline{B}^o_{phys}$] is the state produced as ($q\overline{b}$) [($b\overline{q}$)] at t=0, and $\overline{f} = CP(f)$, are proportional to the expressions:

$$\frac{\Gamma(B^o_{phys} \rightarrow f)}{dt} \propto$$

$$\propto |\langle f|B^o\rangle|^2 e^{-\gamma t}\left\{\left|\cos\frac{\Delta\mu\cdot t}{2}\right|^2 + |\rho|^2\left|\sin\frac{\Delta\mu\cdot t}{2}\right|^2 - 2\,\mathrm{Im}\left[\lambda\,\sin\frac{\Delta\mu\cdot t}{2}\cos^*\frac{\Delta\mu\cdot t}{2}\right]\right\}, \quad (8.1)$$

$$\frac{\Gamma(\overline{B}^o_{phys}\to\overline{f})}{dt}\propto$$

$$\propto |\langle\overline{f}|\overline{B}^o\rangle|^2 e^{-\gamma t}\left\{\left|\cos\frac{\Delta\mu\cdot t}{2}\right|^2+|\overline{\rho}|^2\left|\sin\frac{\Delta\mu\cdot t}{2}\right|^2-2\mathrm{Im}\left[\overline{\lambda}\sin\frac{\Delta\mu\cdot t}{2}\cos^*\frac{\Delta\mu\cdot t}{2}\right]\right\} \quad , \quad (8.2)$$

where we have used (2.8-9) together with the definitions:

$$\lambda\equiv\frac{q}{p}\rho \quad , \quad \overline{\lambda}\equiv\frac{p}{q}\overline{\rho} \quad , \quad \rho\equiv\frac{\langle f|\overline{B}^o\rangle}{\langle f|B^o\rangle} \quad , \quad \overline{\rho}\equiv\frac{\langle\overline{f}|B^o\rangle}{\langle\overline{f}|\overline{B}^o\rangle} \quad , \quad (8.3)$$

while p, q are defined as in (2.4).

We assume $|p/q| \cong 1$ and $\Delta\mu \cong \Delta m \gg \Delta\gamma$ (dominance of top quark in box diagrams), and use time units in which $\tau = 1$. Hence (8.1-2) can be written in the form:

$$\frac{d\Gamma(B^o_{phys}\to f)}{dt} \propto |\langle f|B^o\rangle|^2 e^{-t}\left[\cos^2\frac{x\cdot t}{2}+|\rho|^2\sin^2\frac{x\cdot t}{2}-\mathrm{Im}(\lambda)\sin(x\cdot t)\right] \quad , \quad (8.1')$$

$$\frac{d\Gamma(\overline{B}^o_{phys}\to\overline{f})}{dt} \propto |\langle\overline{f}|\overline{B}^o\rangle|^2 e^{-t}\left[\cos^2\frac{x\cdot t}{2}+|\overline{\rho}|^2\sin^2\frac{x\cdot t}{2}-\mathrm{Im}(\overline{\lambda})\sin(x\cdot t)\right] \quad , \quad (8.2')$$

where, as usual, $x \equiv \Delta m / \gamma$.

The CP violating asymmetry parameter C_f is defined as:

$$C_f \equiv \frac{\Gamma(B^o_{phys}\to f) - \Gamma(\overline{B}^o_{phys}\to\overline{f})}{\Gamma(B^o_{phys}\to f) + \Gamma(\overline{B}^o_{phys}\to\overline{f})} \quad . \quad (8.4)$$

In the Standard Model, violation of CP symmetry is predicted as due to complex coefficients in the CKM matrix.[3] With three generations of quarks, there is only one phase (δ), together with three real rotation angles. The CP violating asymmetries are proportional to $\sin(\delta)$.[28]

Furthermore, it has been proven[29] that any difference in partial width of the kind $[\Gamma(B^o_{phys}\to f)-\Gamma(\overline{B}^o_{phys}\to\overline{f})]$ is proportional to the imaginary part of a combination of coefficient of the CKM matrix, which, in the original parametrization of the matrix, can be written:

$$\Gamma - \overline{\Gamma} \propto s_1^2\, s_2\, s_3\, c_1\, c_2\, c_3 \sin(\delta) \quad , \quad (8.5)$$

where c_i and s_i are cosines and sines of the mixing angles. In the currently preferred parametrization,[24] the same combination of CKM coefficients is parametrized in the form:

$$\Gamma - \overline{\Gamma} \propto s_{12}\, s_{23}\, s_{13}\, c_{12}\, c_{23}\, c_{13}^2 \sin(\delta_{13}) \quad . \qquad (8.5')$$

This theorem establishes the order of magnitude of the numerator in (8.4). It follows that in general the largest asymmetry values are expected for processes with small denominators, i.e. processes with small branching ratios.

In this analysis, we assume that the decays $\Gamma(B^o_{phys} \to f)$ and $\Gamma(\overline{B}^o_{phys} \to f)$ (and the corresponding charge conjugated processes), proceed through one weak diagram only, i.e. through single combinations $V_{ij}V_{kl}^*$ of CKM coefficients. Under this assumption, which should be satisfied to large accuracy in many cases, it can be proven directly [11] that:

$$|\langle f|B^o\rangle| = |\langle f|\overline{B}^o\rangle| \quad , \qquad (8.6)$$

and therefore :

$$|\rho| = |\overline{\rho}| \quad . \qquad (8.7)$$

Using (8.6) in the time integration of (8.1'-2'), the integrated asymmetry is equal to:

$$C_f = \frac{-x\cdot[\mathrm{Im}(\lambda)-\mathrm{Im}(\overline{\lambda})]}{2+x^2+|\rho|^2x^2-\mathrm{Im}(\lambda)-\mathrm{Im}(\overline{\lambda})} \quad . \qquad (8.8)$$

8.1. - Decay to CP-eigenstates

We consider first the case in which the final state is an eigenstate of CP: $f = \pm \overline{f}$, a situation characterized by simplicity in both theory and data analysis.

From (8.3) and (8.6), in this case one obtains:

$$|\rho| = |\overline{\rho}| = 1 \quad . \qquad (8.9)$$

Furthermore the final state phases, due to strong interactions, cancel in the ratios defining ρ, $\overline{\rho}$, while weak phases are opposite for the two terms, hence:

$$\rho = \overline{\rho}^* \quad . \qquad (8.10)$$

We discussed in Sec. 2 that $|p/q|$ is equal to unity to very good approximation, and therefore from the definition (8.3) we find:

$$\lambda = \overline{\lambda}^{*} \quad . \tag{8.11}$$

Replacing these results in (8.1'-2'), the decay distributions are proportional to:

$$e^{-t} \left[1 \pm \mathrm{Im}(-\lambda) \sin (x \cdot t) \right] \quad , \tag{8.12}$$

where x is the oscillation parameter ($\Delta m/\gamma$), the sign (+) correspond to B decays, the (-) to $\overline{B}$.[30] In this case CP violation appears as a non vanishing value of Im(λ), with a departure from an exponential decay law. Notice that $|\lambda| = 1$, and large C_f values may be present in these decays.

8.2. - Decay to CP-non-eigenstates

In the most general case, we consider the four cases of B^o_{phys} , $\overline{B}^o_{phys}$ decaying into f , $\overline{f}$. From (8.1'-2'), the definitions (8.3), and (8.6), the decay distributions are given by:

$$\frac{d\Gamma(B^o_{phys} \to f)}{dt} \propto |\langle f|B^o\rangle|^2 e^{-t} \left[\cos^2 \frac{x \cdot t}{2} + |\rho|^2 \sin^2 \frac{x \cdot t}{2} - \mathrm{Im}(\lambda) \sin(x \cdot t) \right] , \tag{8.13}$$

$$\frac{d\Gamma(\overline{B}^o_{phys} \to \overline{f})}{dt} \propto |\langle f|B^o\rangle|^2 e^{-t} \left[\cos^2 \frac{x \cdot t}{2} + |\rho|^2 \sin^2 \frac{x \cdot t}{2} - \mathrm{Im}(\overline{\lambda}) \sin(x \cdot t) \right] , \tag{8.14}$$

$$\frac{d\Gamma(\overline{B}^o_{phys} \to f)}{dt} \propto |\langle f|B^o\rangle|^2 e^{-t} \left[|\rho|^2 \cos^2 \frac{x \cdot t}{2} + \sin^2 \frac{x \cdot t}{2} + \mathrm{Im}(\lambda) \sin(x \cdot t) \right] , \tag{8.15}$$

$$\frac{d\Gamma(B^o_{phys} \to \overline{f})}{dt} \propto |\langle f|B^o\rangle|^2 e^{-t} \left[|\rho|^2 \cos^2 \frac{x \cdot t}{2} + \sin^2 \frac{x \cdot t}{2} + \mathrm{Im}(\overline{\lambda}) \sin(x \cdot t) \right] . \tag{8.16}$$

The parameter λ can be expressed by:

$$\lambda = |\rho| \, e^{i(\phi + \chi)} \quad , \tag{8.17}$$

where the phase ϕ is due to weak interactions, and includes the ratios of the CKM combinations entering in the definition of ρ (8.3) and the phase of (q/p), while χ comes from the final state phases. The corresponding expression for $\overline{\lambda}$ is :

$$\overline{\lambda} = |\rho| \, e^{i(-\phi + \chi)} \quad , \tag{8.18}$$

since in the charge conjugated process the phases of the CKM coefficients are opposite, (q/p) is replaced by (p/q), while the final state phases are the same. It follows that the interference terms in (8.13-16) are given by:

$$- |\rho| \sin(\chi+\phi) \sin(x\cdot t) \quad , \tag{8.19}$$

$$- |\rho| \sin(\chi -\phi) \sin(x\cdot t) \quad , \tag{8.20}$$

$$+ |\rho| \sin(\chi+\phi) \sin(x\cdot t) \quad , \tag{8.21}$$

$$+ |\rho| \sin(\chi -\phi) \sin(x\cdot t) \quad . \tag{8.22}$$

For $\chi \neq 0$, the interference terms may be present even in the absence of CP violation ($\phi=0$). Notice that the CP violating effects result proportional to $\cos(\chi)$.

Expressions (8.19-22) can be simplified if the quark fragmentation into the final state proceeds through a single strong interaction channel. Under this assumption, only one final state phase enters in the numerators and denominators defining ρ and $\overline{\rho}$, hence resulting in vanishing χ. The interference terms are therefore proportional to:

$$\pm |\rho| \sin(\phi) \sin(x\cdot t) \tag{8.23}$$

where the sign (+) applies to decays (8.14-15), and the sign (-) to (8.13, 8.16). Under these approximations, the interference term is evidence for CP violation.

9. - DETECTION OF CP VIOLATION

The detection of CP violating effects has been beyond the capability of any experimental study of beauty physics performed until now. In this section we discuss the sensitivity necessary to detect such effects. We evaluate the statistical uncertainty in some detail, and discuss some major systematic effects, such as those due to inclusive tagging, tagging inaccuracy and decay time limited resolution.

We shall first consider measurements based on time integrated techniques, then analyses of decay time distributions.

9.1. - Time integrated analysis

For any reaction $B^o_{phys} \to f$, $\overline{B}^o_{phys} \to \overline{f}$, the asymmetry C_f (8.4) can be obtained measuring the ratio:

$$C_f = \frac{N(B^o_{phys} \to f) - N(\overline{B}^o_{phys} \to \overline{f})}{N(B^o_{phys} \to f) + N(\overline{B}^o_{phys} \to \overline{f})} \quad . \tag{9.1}$$

From this expression, the statistical uncertainty is given by:

$$\sigma_{C_f} = 2\sqrt{\frac{1-C_f^2}{N_{f/\overline{f}}}} \quad , \tag{9.2}$$

where $N_{f/\overline{f}}$ is the total number of decays in the denominator of (9.1).

Table II shows estimates of $|\rho|^2$, $\mathrm{Im}(\lambda)$ and C_f for the different quark subprocesses, computed according to the assumptions on the CKM angles shown in Table III, which are consistent with the experimental constraints.[2] The phase δ was set at the value which maximizes CP violating effects. Analytical expressions for $|\rho|^2$ and $\mathrm{Im}(\lambda)$ are provided in Ref. 11. Notice that the effects of strong interactions are neglected, implying $\chi=0$ in (8.17-18), and ignoring correction to the value of $|\rho|^2$. This is expected to be a reasonable approximation if the final state is a single eigenstate of strong interactions, and if the four decays involved in the analysis proceed through quark diagram of the same kind ("spectator", "exchange" or "penguin").[11] For the B_s-$\overline{B}_s$ system, we considered three cases, corresponding to values of the oscillation parameter x_s equal to 5, 10 and 15. Table II shows that the asymmetry values in the B_s-$\overline{B}_s$ system are typically smaller than those in the B_d-$\overline{B}_d$ system. This is due to the dependence of C_f on x, as shown in (8.8): the asymmetry vanishes for x=0, but also decreases as 1/x for $x \gg 1$.

Notice that this measurement requires the identification of the beauty quantum number at production time ("tagging"), in the same way as discussed in Sections 3-4 for the measurement of flavor oscillation. Erroneous tagging will reduce the apparent C_f value by the factor α_2 of (4.2). If inclusive tagging will be used, the apparent signal will be also reduced by the factor α_1 of (3.6).

If the final state is a CP eigenstate, under the approximation of (8.9,8.11) discussed above, the asymmetry C_f can be related directly to the phase ϕ, according to the equation:

$$C_f = -\frac{x}{1+x^2}\sin(\phi) \quad . \tag{9.3}$$

In the most general case (final state CP-non-eigenstate), the measurement of the four decay widths of (8.13-16) can be used to determine $|\langle f|B^o\rangle|^2$, $|\rho|^2$, and the phases ϕ, χ defined in (8.17-18).

We show below some example of statistical sensitivity typical of this method, in comparison with results based on decay distribution analysis.

9.2. - Decay time distributions analysis

We have used a Monte Carlo to generate samples of decay times corresponding to the four processes of (8.13-16). The simulation assumed a decay proper time resolution equal to $0.1\cdot\tau$, which reduces the apparent amplitude of the oscillating terms in the decay distributions by the factor α_3 of (4.5). A further reduction is due to erroneous determination of the beauty number at production time, i.e. tagging errors, or tagging on oscillating partners. We assumed the overall tagging inaccuracy equal to 25% (i.e. we set the product of the coefficients α_1 and α_2 (3.6, 4.2) equal to 0.5 [31]).

Samples of tagged decay times were analyzed using the maximum likelihood method.[23] Only events with (smeared) decay time larger than $0.5\cdot\tau$ were used, and we assumed that the detection efficiency for events satisfying this cut does not depend on the decay time ($\varepsilon(t)$ is assumed constant for $t > 0.5\cdot\tau$).

Our analysis assumed the values of τ , x , $\alpha_1\cdot\alpha_2$, σ_t , $\varepsilon(t)$, as fixed, i.e. as pre-determined quantities. This assumption is justified by the fact that they can be measured by independent analyses based on larger samples of more copious decay channels, in some cases not subjected to the tagging requirement. However, in order to test the reliability of the technique, we performed a few fits with systematic offsets in the values of $\alpha_1\cdot\alpha_2$, and x used in the fitting algorithm.

Neglecting the background due to events with different τ or x values should instead be considered as a general feature of our analysis, which assumes fully reconstructed B-mesons, in the same way as discussed above in Sec.'s 3-6 for the measurement of x_s.

The analysis was repeated for values of the oscillation parameter x equal to 0.7 (B_d), 5 , 10 and 15 (covering a range expected for B_s). Each analysis was repeated 15 times on independent samples to evaluate systematic effects and the uncertainties on the results of a single analysis. We found that the technique is essentially unbiased, apart from minor ef-

fects pointed out below, providing good estimates of the generated values and of the resolution achieved in the fitted variables.

Different statistical sample sizes were used, ranging from 100 to 1000 events. We directly checked that the usual $1/\sqrt{N}$ behavior of the statistical error is satisfied, and we show results for samples of 1000 events. This number includes B and $\overline{B}$ events, as discussed below. We looked for maxima of the likelihood away from the generated values of the fitted parameters, but they were not found, at least for sample size large enough to provide measurement of the interference term with more than 2 σ significance. The generated values of the fitted quantities were taken from Table II.

9.2.1. - Results for CP-eigenstate final states

We performed a one variable fit to the value of the parameter $\mathrm{Im}(\lambda) \equiv \sin(\phi)$.[32] The generated value was set equal to -.8 . This choice is representative of the decays $B_d \to D^+D^-$, $D_S\overline{D}_S$, ψK_S, ϕK_S, ψF, $\pi^+\pi^-$, K^+K^-, and $B_s \to D_S\overline{D}_S$, D^+D^-, ψF, ψK_S, $\pi^o K_S$, K^+K^-, $\pi^+\pi^-$, ϕK_S . Fig. 3 shows the decay distributions for these processes and the corresponding charge conjugated ones, with the oscillation parameter x set at 0.7 and at 10.

The relative abundance of B and $\overline{B}$ events was determined by the decay probabilities, assuming equal production cross section. Table IV shows the statistical resolution achieved in $\sin(\phi)$. For comparison, the expectation for a time-integrated analysis is shown. For x=0.7 (B_d) the advantage of a time-dependent approach is only apparent: we found that the better resolution is due to the requirement: $t > 0.5 \cdot \tau$; if the same requirement were placed on events entering the ratio (9.1), (9.3) would be modified, and the resulting resolution in the variable $\sin(\phi)$ would result equal to the one achieved by the time dependent analysis, for equal samples of events entering the analysis. On the other hand, for $x \geq 5$, much larger sample sizes are necessary to detect the CP violating term with time integrated methods.

9.2.2. - Results for final states with a single strong eigenchannel

In this case, the variables $|\rho|^2$ and $\sin(\phi)$ were fitted at the same time. We generated samples with the first parameter set at 5., and the second at -.9 . These values are expected for the cases involving $B_d \to D^o K_S$, $B_s \to D^+\pi^-$, $D^o\pi^o$, $D_S K^-$, $D^o\phi$ and the charge conjugated processes. Because of tagging errors, in a real measurement the collected sample would contain also events with charge conjugated initial state and same final state (for

example: $B_s \to D^- \pi^+$ and $\overline{B}_s \to D^+ \pi^-$), which correspond to $|\rho|^2=0.2$. In our analysis, we generated both kinds of events, corresponding to the four different decay distributions (8.13-16).

The relative abundance of the different cases was fixed assuming equal production cross section for B and $\overline{B}$, and accounting for the different decay probabilities to the final states. Fig. 4 shows the decay distributions corresponding to the four channels, for values of x equal to 0.7 and 10. The normalization of the vertical axis is equal in all the plots. Table V shows the resolution values obtained in the simulated analysis, The requirement: $\sin(\phi) \geq -1$ produced a minor bias in the average $\sin(\phi)$ fitted value, in the range 0.0-0.2, always smaller than the average rms uncertainty by at least a factor two. The errors shown include the effect of correlation between the two variables. The averages of the absolute values of the correlation coefficients were found in the range 0.1 to 0.4 .[33]

9.2.3. - Results for final states with "strong" interference

As discussed above in Sec. 8.2, in the most general case the interference term in the decay distribution depends on a phase χ characteristic of the final state, determined by strong interactions (8.19-22). Notice that CP violating asymmetries result proportional to $\cos(\chi)$. We generated Monte Carlo events with $|\rho|^2=5$, $\phi=\pi/2$, $\chi=0.35$.

Since the two phases are measured only through the values of $\sin(\chi \pm \phi)$, eight equivalent solutions are found within the range $-\pi$ to $+\pi$ (see Fig. 5).[34] Therefore the measurement of the decay distributions alone cannot fully constrain the value of ϕ (or χ). In order to select a single solution, the algorithm examined only the area of the $\chi \cdot \phi$ plane satisfying: $-\pi/2 \leq \chi \pm \phi \leq +\pi/2$. In our case, the resulting values are $\phi=1.22$, $\chi=0$. For these values, the decay distributions are very similar to those shown in Fig. 4.

Table VI shows the resolution obtained in the three variables, with correlation effects included. Notice that the fitted ϕ value is not far from its upper bound, hence the statistical error σ_ϕ is not symmetric. The last column shows the corresponding negative side error in the variable $\sin(\phi)$.

9.2.4. - Sensitivity to the values of fixed parameters

In order to evaluate whether our results depend critically on the assumptions of accurate knowledge of the parameters kept constant in the optimization algorithm, we analyzed the data generated at x=10 with modified values of x, and, independently, of the product

$\alpha_1 \cdot \alpha_2$. With x set at 10.25, the results of the fit were not affected in any significant way. Notice that in this way we also proved that a 2.5% systematic error in the lifetime value used in the analysis can be neglected. Using $\alpha_1 \cdot \alpha_2 = 0.6$ rather than 0.5, we obtained a $\approx$20% reduction in the fitted values of $\sin(\phi)$, $|\rho|^2$, and also in the corresponding uncertainties.

10. - CONCLUSIONS ON CP VIOLATION

From the results of the previous section, it appears that a total sample of the order of 1000 events in the decay channels: $B^o \to f$, $B^o \to \overline{f}$, $\overline{B}^o \to f$, $\overline{B}^o \to \overline{f}$ can provide a statistical resolution in the CP violating term $\mathrm{Im}(\lambda)$ in the range 0.1-0.4 . The resolution depends on the process examined (decay into CP eigenstates are favored, while final state phases interference introduces ambiguities), on the value of oscillation parameter ($x \approx 5$ is more favorable that $x \approx 1$) and on the detector quality factors (mistagging and decay time resolution). For detector characteristics different from those considered in this analysis, our results can be approximately corrected by scaling the resolution $\sigma_{\sin(\phi)}$ according to $1/\alpha$, where $\alpha = \alpha_1 \cdot \alpha_2 \cdot \alpha_3$ takes into account erroneous tagging and limited decay time resolution according to (3.6), (4.2) and (4.5).

Notice that the required statistical sample size is of the same order of the one necessary for measuring x_s, discussed in Sec.'s 5. However, the detection of CP violation is much more demanding in the number of $b\text{-}\overline{b}$ quark pairs. In fact, in the case of mixing study we can select decay channels with relatively large branching ratios (and therefore small CP asymmetries), and sum them together. We discussed in Sec. 6 that $\approx$2% of the B_s decay channels are potentially available for this analysis. On the other hand, in order to detect CP violations, in general we must analyze exclusive decay channels separately, since strong interactions will affect each case differently. Different decays can be analyzed together only if the final states are CP eigenstates, and the decays involve the same dominant quark transition, since in this case the effects of strong interactions cancel in the amplitude ratios ρ, $\overline{\rho}$ (8.3).

If the final state is not a CP eigenstate, in order to avoid the ambiguity of measuring at the same time the interference terms due to the CKM matrix and the final state phases, we have to limit the analysis to final states which are single eigenstate of strong interactions. Therefore we must restrict our choice to two body final states, selecting those where a single quark diagram can be drawn.

The expected branching ratios, for channels with relatively large CP violating interference terms, are in the range 10^{-5}-10^{-3}.[11] For the same efficiency assumptions of Sec. 6, and including the branching ratios of B-decay products into favorable final states (for instance: $J/\Psi \rightarrow e^+e^-$ or $\mu^+\mu^-$) it appears that samples of the order of 10^8 recorded $b\text{-}\overline{b}$ pairs are needed to study CP violation in the neutral B-mesons.

Concerning the relevance of decay time analysis, our results show that while the measurement of CP violation in the B_d-$\overline{B}_d$ system may not require this technique, on the other hand the analysis of decay time distributions will probably be a necessary tool in the measurement of CP violation in the B_s-$\overline{B}_s$ system. For $x_s \approx 5$ or larger, and $\sigma_t < \tau / x_s$, the measurement might result less demanding in the B_s-$\overline{B}_s$ system. The detection of CP asymmetries in the two cases, particularly if found in several decay processes, will obviously allow a comprehensive test of our understanding of the weak interactions and of the source of CP violation.

Acknowledgments. We are grateful to R. Cester at University of Torino, G. Borreani at University of Ferrara, S. Erhan, M. Medinnis, P. Schlein and J. Zweizig at University of California, Los Angeles, and V. Obraztsov at IHEP-Serpukhov for useful discussions concerning the subject of this report.

REFERENCES

(1) For a review see: H. Schroeder, Rep. Prog. Phys., **52**, 765 (1989).

(2) F. J. Gilman, K. Kleinknecht and B. Renk, SLAC Report, SLAC-PUB-5155 (1989).

(3) N. Cabibbo, Phys. Rev. Lett. **10**, 531 (1963); M. Kobayashi and T. Maskawa, Prog. Theor. Phys. **49**, 652 (1973).

(4) H. Albrecht et al. (ARGUS Coll.), Phys. Lett. **192B**, 245 (1987); A. Bean et al. (CLEO Coll.), Phys. Rev. Lett. **58**, 183 (1987).

(5) For reviews and references to previous work see: G. Altarelli, CERN Report, CERN-TH-4896 (1987); A. Fridman, CERN Report, CERN-EP/88-123 (1988), K. R. Schubert, Progr. in Part. and Nucl. Phys., **21**, 3 (1988).

(6) P. J. Franzini, Phys. Rep. **173**, 1 (1989).

(7) P. Krawczyk, D. London and H. Steger, DESY Report, DESY 88-163 (1988).

(8) P. Roudeau, LAL-Orsay Report, LAL 89-21 (1989); D. Treille, CERN Report, CERN-EP/89-90 (1989).

(9) For a review and references to previous work see: K. J. Foley et al., Proceed. Workshop on Experiments, Detectors and Experimental Areas for the Supercollider, Berkeley, July 7-17, 1987, ed. R. Donaldson and M. G. Gilchriese, World Scientific, Singapore, 1988, p.701.

(10) L. L. Chau and H. Y. Cheng, Phys. Lett. **165B**, 429 (1985); M. Bander, D. Silverman and A. Soni, Phys. Rev. Lett. **43**, 242 (1979).

(11) I. Dunietz and J. L. Rosner, Phys. Rev. **D34**, 1404 (1986).

(12) If we adopt the definition: $CP(B^o) = \overline{B}^o$, $CP(\overline{B}^o) = B^o$, then in the approximations of (2.12) B_H and B_L are CP eigenstates, and (2.13) implies: $CP(B_L) = + B_L$, $CP(B_H) = - B_H$.

(13) G. Altarelli and P. J. Franzini, Z. Phys. C-Particles and Fields **37**, 271 (1988).

(14) A. Pais and S. B. Treiman, Phys. Rev. **D12**, 2744 (1975).

(15) Under the assumptions of $B^{\pm}$ tagging taken above, R = r. In case of B^o-$\overline{B}^o$ production, oscillations of both particles, and coherence effects must be taken into account, and $R \neq r$ unless the mesons are produced in an odd angular momentum state, like $Y(4S) \rightarrow B_d\text{-}\overline{B}_d$. See Ref. 4, 6, and I. I. Bigi and A. I. Sanda, Nucl. Phys. **B193**, 85 (1981).

(16) It has been proposed to build asymmetric electron-positron colliders, operating at the Y-family resonances, where the center-of-mass frame is in motion with respect to the laboratory frame. This allows the B-mesons to move before decaying. In practice, because of the relatively large length of the interaction region, only the de-

cay time difference between the two members of a pair is experimentally accessible. See: PSI asymmetric collider proposal, PSI Report, PR-88-09 (1988); J. Rees, SLAC Report, SLAC/AP-67 (1988); H. Nesemann et al., DESY Report, DESY 89-080 (1989).

(17) W. Bartel et al.(JADE Coll.), Phys. Lett. **146B**, 437 (1984); T. Schaad et al. (MARK II Coll.), Phys. Lett. **160B**, 188 (1985); H. R. Band et al. (MAC Coll.), Phys. Lett. **200B**, 221 (1988).

(18) C. Albajar et al. (UA1 Coll.), Phys. Lett. **186B**, 247 (1987)

(19) A. Brandt et al., CERN Report, CERN-SPSC/89-43 (1989)

(20) These ratios are based on common quark fragmentation assumptions. See F. E. Paige and S. Protopopescu, BNL Report BNL-38034 (1986), for a discussion in the framework of the ISAJET Monte Carlo.

(21) A different approach would limit the reconstruction to the determination of a secondary vertex, without full secondary identification and invariant mass calculation. Leptonic tagging would be applied on both members of a pair. Notice that errors in associating tracks with primary and secondary vertices increase the effective σ_t. The decay time analysis requires the subtraction of non oscillating B_u, Λ_b, slowly oscillating B_d and maybe also of charmed particles background. The time integrated version of this approach provided evidence of B^o-$\overline{B}^o$ mixing, without separating B_d's and B_s's (see Ref. 18).

(22) A. Brandt et al., CERN Proposal P238, CERN Report, CERN-SPSC/88-33 (1989); CERN-SPSC/89-55 (1989); CERN SPSC/89-61 (1989);

(23) F. James and M. Roos, MINUIT Package, CERN Computer Centre Program Library.

(24) Review of Part. Properties, Phys. Lett. **B204** (1988).

(25) The efficiency values considered here are larger than those achieved in the experiments which so far succeeded in fully reconstructing B-mesons (see Ref. 1). However, those experiment took data at the Y(4S) resonance, with B-mesons at rest, while here we are assuming that reliable vertex separation is achieved, obtaining a larger reconstruction efficiency. We approximately follow the results of a simulation discussed in Ref. 19, 22.

(26) H. Castro et al., BCD Collaboration Letter of Intent, FNAL (1988).

(27) I. I. Bigi and A. I. Sanda, Nucl. Phys. **B281**, 41 (1987).

(28) Notice that constraints on δ could be obtained independently from CP violating effects, since $\cos(\delta)$ is related to x_s, as shown by (2.17), with the coefficients of the CKM matrix expressed in terms of the four angles. However, even assuming that x_s could be measured with accuracy comparable to the values discussed in this re-

port, a significant bound on $\cos(\delta)$ requires improvements in the measurements of the mixing angle between the first and the third generation, and, to a larger extent, of the oscillation parameter x_d. See Ref. 8.

(29) C. Jarslkog, Phys. Rev. Lett. **55**, 1039 (1981); Z. Phys. C.-Particles and Fields **29**, 491 (1985).

(30) Expression (8.12) is valid for CP(f)=+f. If f is CP odd, λ should be multiplied by a factor (-1), as discussed in Ref. 11.

(31) In case of decays to CP eigenstates, the effects of α_1 and α_2 can be included in the definition of an effective value of $\mathrm{Im}(\lambda)$, simplifying the formalism used in the analysis. (And with some generalization, for small σ_t values, α_3 could also be included). However, in the most general case, $|\rho|^2$ is affected differently by the oscillation reducing coefficients, and we prefer to use the most general notation.

(32) In a different notation, $\lambda \equiv \exp(2i\Phi)$, where the phase Φ can be identified with one of the inner angles of the "unitarity triangle"; see for instance J. L. Rosner, A. I Sanda, and M. P. Schmidt, Proceed. Workshop on High Sensitivity Beauty Physics at Fermilab, 1987, ed. A. J Slaughter, N. Lockyer, and M. Schmidt, Fermilab, Batavia, 1985, p. 165; F. J. Gilman, SLAC Report, SLAC-PUB-5018 (1989).

(33) We did not analyze the quark sub-processes with $|\rho|^2=1800$, and $|\rho|^2=5.6\cdot10^{-4}$ because of the small size of $|\mathrm{Im}(\lambda)| / (1+|\rho|^2)$ (See Table II). The detection of CP violation would result more difficult, despite the branching ratios are estimated to be typically larger in this case (see Ref. 11).

(34) Apart from the obvious symmetry operation $(\chi,\phi)\rightarrow(\chi+2n\cdot\pi,\phi+2m\cdot\pi)$ with n, m integer, the solutions are symmetric under the transformations: $(\chi,\phi)\rightarrow(\chi+\pi,\phi+\pi)$, $(\chi,\phi)\rightarrow(\pi-\chi,-\phi)$, $(\chi,\phi)\rightarrow(\pi/2-\phi,\pi/2-\chi)$. The last transformation is used in the example reported in the text.

TABLES

TABLE I. - Results of the simulated analysis for the resolution σ_x in the oscillation parameter; x is the generated value of the oscillation parameter, σ_t is the experimental uncertainty in the decay time, $\alpha_1 \cdot \alpha_2$ describes the tagging accuracy, N is the statistical sample, Δ_S provides the separation of spurious solutions.

x	σ_t/τ	$\alpha_1 \cdot \alpha_2$	N	σ_x	Δ_S
1.	.07	0.8	40	.16(±.04)	3.4(±1.3)
1.	.07	0.8	100	.09(±.01)	6.0(±0.6)
5.	.07	0.8	40	.16(±.05)	2.8(±1.4)
5.	.07	0.8	100	.12(±.02)	5.2(±1.1)
15.	.07	0.8	40	.21(±.06)	0.7(±2.6)
15.	.07	0.8	100	.18(±.03)	1.3(±1.2)
1.	.20	0.8	40	.14(±.02)	3.2(±1.0)
1.	.20	0.8	100	.09(±.02)	5.1(±0.7)
5.	.20	0.8	40	.22(±.07)	2.2(±1.1)
5.	.20	0.8	100	.21(±.09)	3.9(±0.8)
5.	.07	0.3	1400	.08(±.02)	5.3(±0.5)
5.	.07	0.3	2800	.05(±.01)	8.1(±1.1)
15.	.07	0.3	1400	.08(±.03)	3.6(±1.1)
15.	.07	0.3	2800	.07(±.02)	4.8(±0.8)

TABLE II. - Values of decay distribution parameters and integrated asymmetry C_f for the different quark processes. The CKM angles are set at the values given in Table III. The phase δ is set at $\pi/2$ - (*) with the exception of the first process, where it is set at $\pi/4$. The fourth column, $|\mathrm{Im}(\lambda)/(1+|\rho|^2)|$, shows the relative magnitude of the CP violating interference term.

Decay channel	$\lvert\rho\rvert^2$	$\mathrm{Im}(\lambda)$	$\frac{\lvert\mathrm{Im}(\lambda)\rvert}{1+\lvert\rho\rvert^2}$	C_f		
		B_d-$\overline{B}_d$		(x_d=0.7)		
$\overline{b} \to \overline{u}u\overline{d}, \overline{u}u\overline{s}$ (*)	1.	-1.	.5	.47		
$\overline{c}c\overline{s}, \overline{u}u\overline{s}, \overline{s}$	1.	-.80	.40	.38		
$\overline{d}$	1.	0.	0.	0.		
$\overline{u}c\overline{s}$	5.0	-2.0	.33	.57		
$\overline{c}u\overline{s}$	.20	-.40	.33	.22		
$\overline{u}c\overline{d}$	1800	38	.021	-.060		
$\overline{c}u\overline{d}$	$5.6\cdot10^{-4}$	.021	.021	-.012		
		B_s-$\overline{B}_s$		(x_s=5	10	15)
$\overline{b} \to \overline{u}u\overline{d}, \overline{u}u\overline{s}$	1.	-.80	.40	.15	.079	.053
$\overline{c}c\overline{s}, \overline{c}c\overline{d}$	1.	.042	.021	-.0081	-.0042	-.0028
$\overline{d}$	1.	.80	.40	-.15	-.079	-.053
$\overline{s}$	1.	0.	0.	0.	0.	0.
$\overline{u}c\overline{s}$	5.0	-2.0	.33	.13	.066	.044
$\overline{c}u\overline{s}$	.20	-.40	.33	.13	.066	.044
$\overline{u}c\overline{d}$	1800	38	.021	-.0084	-.0042	-.0028
$\overline{c}u\overline{d}$	$5.6\cdot10^{-4}$	.021	.021	-.0078	-.0041	-.0028

TABLE III. - Values of the sines of the CKM angles used in this analysis, shown in the original parametrization and the parametrization of Ref. 24.

$s_1 = 0.22$	$s_2 = 0.05$	$s_3 = 0.025$
$s_{12} = 0.22$	$s_{23} \equiv 0.056$	$s_{13} \equiv 0.0055$

TABLE IV. - Resolution in the interference term for different values of the oscillation parameter, with rms errors. The analyzed sample is 1000 events. The third column shows the resolution obtained with time integrated analysis.

x	$\sigma_{\sin(\phi)}$	σ(t.i.)
0.7	.18(±.02)	.26
5.	.096(±.002)	.65
10.	.132(±.003)	1.28
15.	.243(±.005)	1.90

TABLE V. - Resolution in the fitted parameters in the case of no interference between final state phases.

x	$\sigma_{\lvert\rho\rvert^2+}$	$\sigma_{\lvert\rho\rvert^2-}$	$\sigma_{\sin(\phi)}$
0.7	+2.4(±1.5)	-1.5(±.9)	.23(±.07)
5.	+2.4(±1.0)	-1.5(±.6)	.13(±.04)
10.	+3.8(±1.7)	-2.0(±.9)	.21(±.05)
15.	+6.6(±2.0)	-3.8(±1.1)	.36(±.08)

TABLE VI. - Resolution in the fitted parameters in the most general case of interference due to CP violation and final state phases. The generated ϕ value is 1.22 rad.

x	$\sigma_{\|\rho\|^2+}$	$\sigma_{\|\rho\|^2-}$	σ_χ	$\sigma_{\phi+}$	$\sigma_{\phi-}$	$\sigma_{\sin(\phi)-}$
0.7	+2.6(±1.3)	-1.5(±.7)	.38(±.11)	+.28(±.21)	-.42(±.07)	-.22(±.08)
5.	+2.0(±.8)	-1.3(±.5)	.27(±.09)	+.25(±.10)	-.28(±.08)	-.13(±.05)
10.	+3.1(±1.8)	-1.8(±1.0)	.33(±.11)	+.30(±.17)	-.38(±.07)	-.20(±.08)
15.	+6.(±2.)	-4.(±1.)	.51(±.13)	+.33(±.18)	-.57(±.13)	-.33(±.10)

FIGURES

FIG. 1. - Box diagrams determining the B^o-$\overline{B}^o$ amplitude.

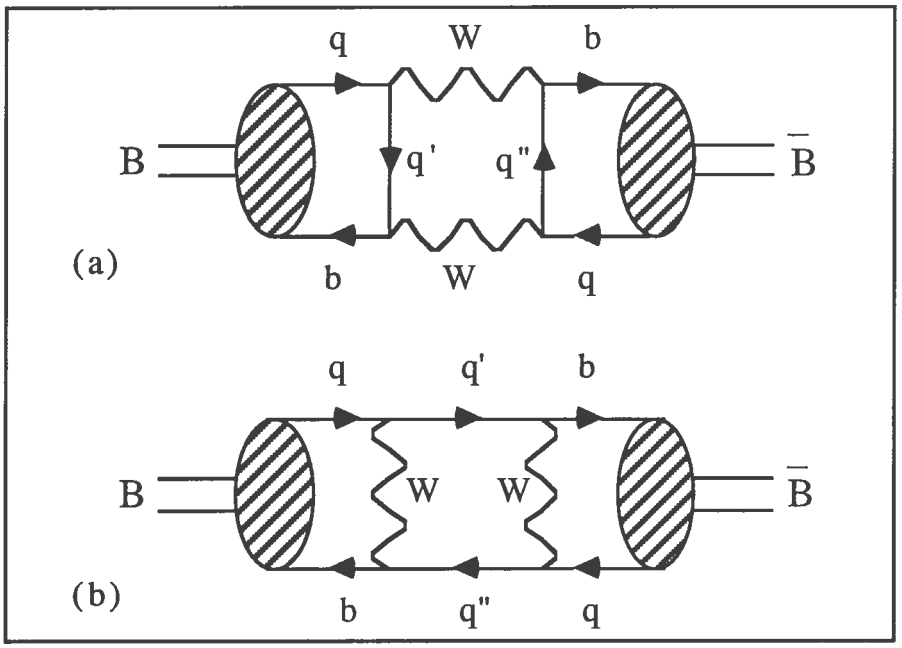

FIG. 2 - Decay distributions (in lifetime units) corresponding to flavor conservation (continuous lines) and flavor oscillation (dotted lines) for (a): x=0.7 , (b): x=10.

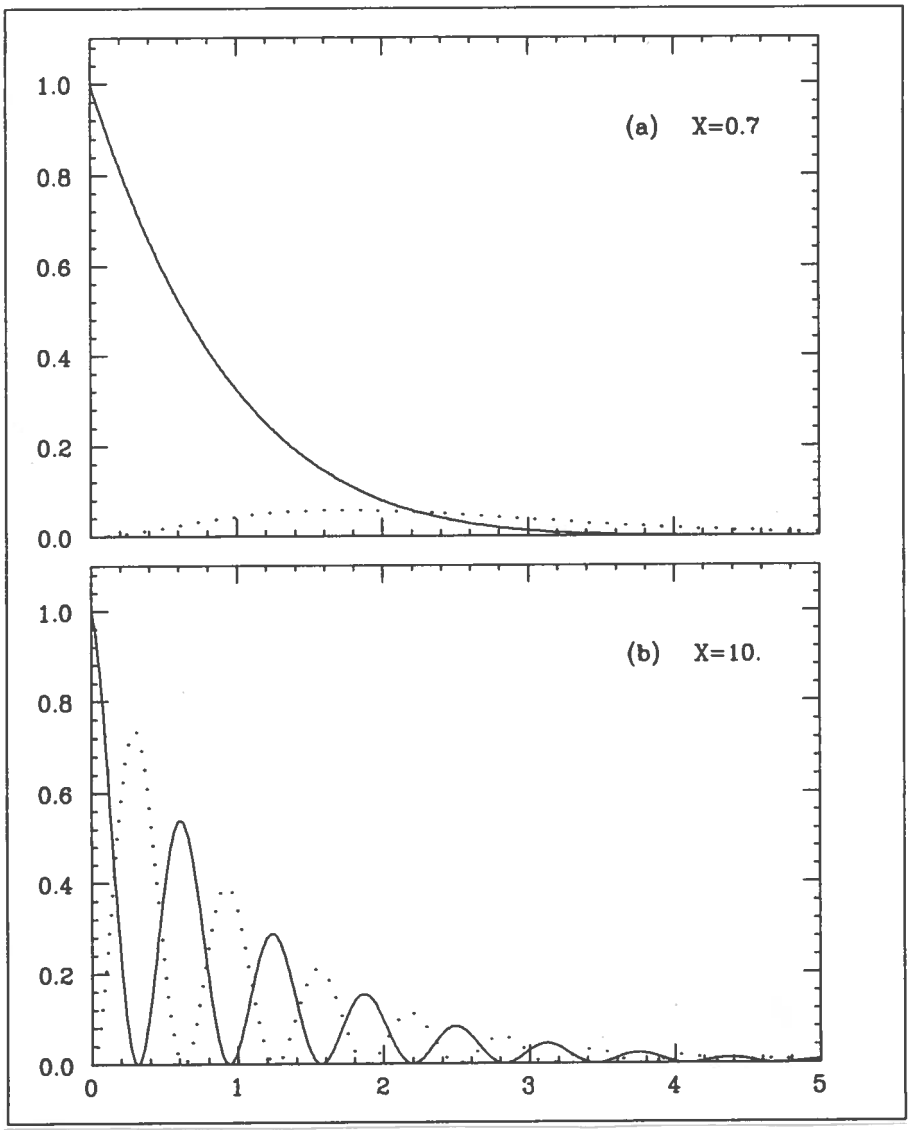

FIG. 3 - Decay distributions (in lifetime units) for $B^0_{phys} \to f$ (continuous lines) and $\overline{B}^0_{phys} \to f$ (dotted lines), for CP(f)=+f , Im(λ)=-0.8 , and (a): x=0.7 , (b): x=10 .

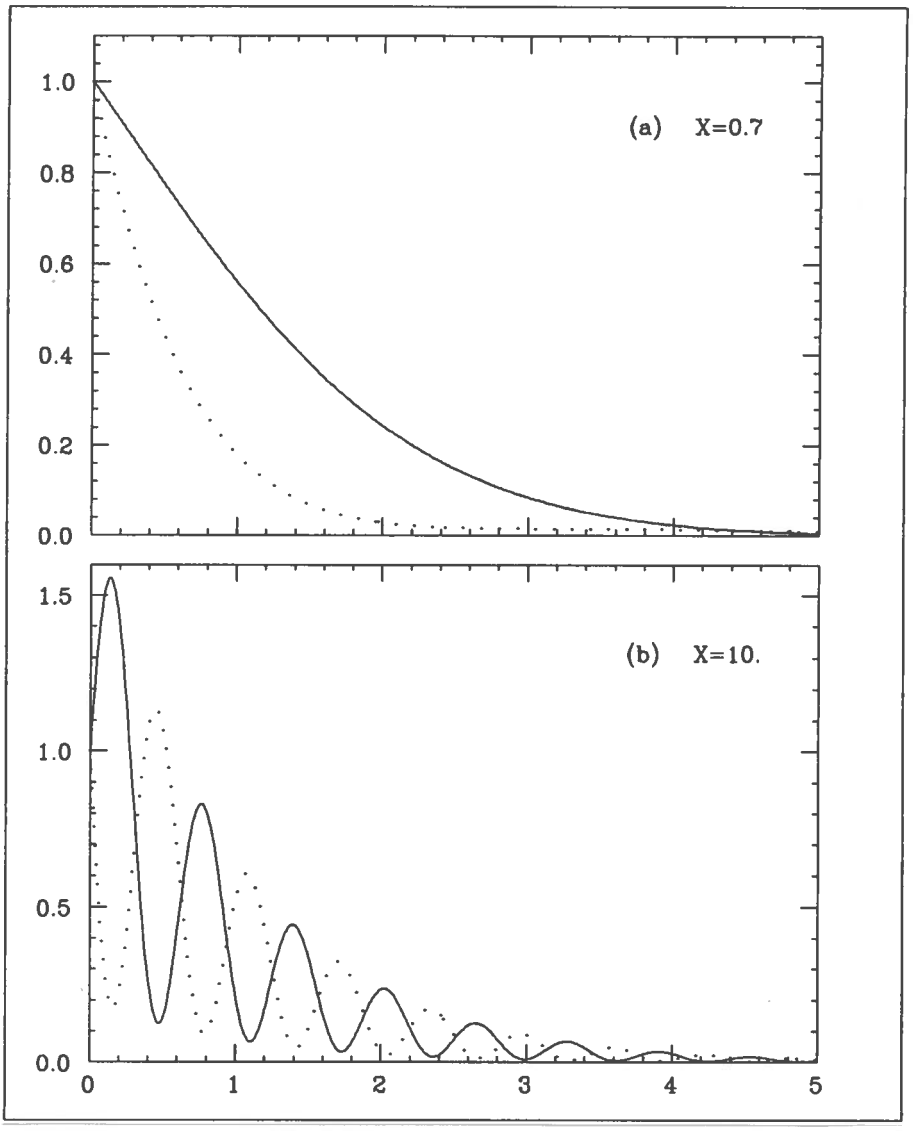

FIG. 4 - Decay distributions (in lifetime units) for $|\rho|^2=5.0$, $\mathrm{Im}(\lambda)=-2.0$, $x=0.7$; (a) : $B^o_{phys}\to f$ (continuous line), $\overline{B}^o_{phys}\to\overline{f}$ (dotted line); (b) : $\overline{B}^o_{phys}\to f$ (continuous line), $B^o_{phys}\to\overline{f}$ (dotted line); (c-d) : same as above for $x=10$. Since $|\rho|>1$ decays (a,c) are favored over the corresponding (b,d) (the vertical axis normalization is the same in the four plots).

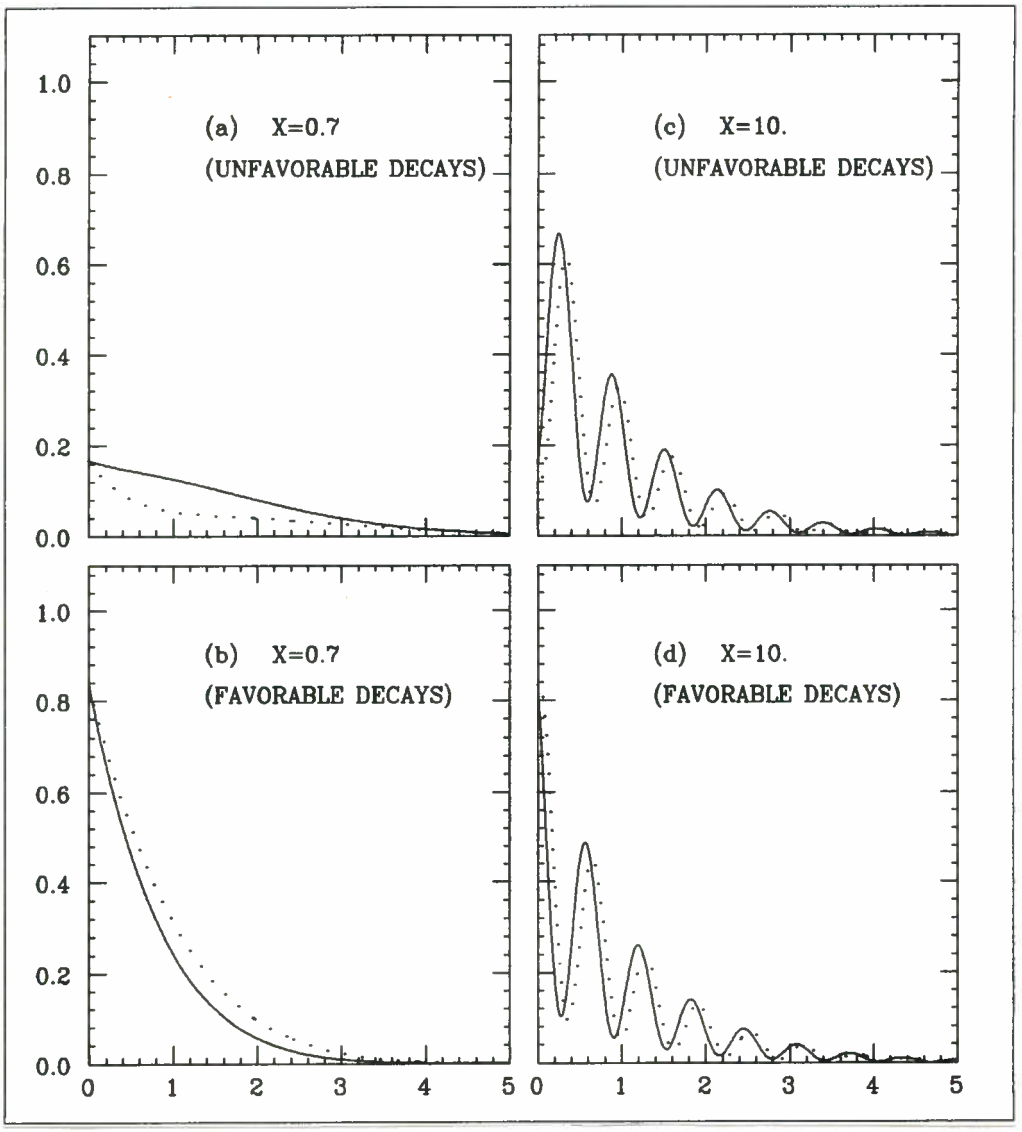

FIG. 5 - Values of (χ,ϕ) corresponding to the example considered in the analysis simulation. Lines of constant $(\chi\pm\phi)$ are drawn; a single solution is found in the central region.